NeuroImage: Clinical 26 (2020) 102225

Contents lists available at ScienceDirect

NeuroImage: Clinical

journal homepage: www.elsevier.com/locate/ynicl

Motor effects of deep brain stimulation correlate with increased functional connectivity in Parkinson's disease: An MEG study

Lennard I. Boon [a, b, *], Arjan Hillebrand [b], Wouter V. Potters [c], Rob M.A. de Bie [c], Naomi Prent [c], Maarten Bot [d], P. Richard Schuurman [d], Cornelis J. Stam [b], Anne-Fleur van Rootselaar [c], Henk W. Berendse [a]

[a] Amsterdam UMC, Vrije Universiteit Amsterdam, Neurology, Amsterdam Neuroscience, De Boelelaan 1117, Amsterdam, the Netherlands
[b] Amsterdam UMC, Vrije Universiteit Amsterdam, Clinical Neurophysiology and Magnetoencephalography Centre, Amsterdam Neuroscience, De Boelelaan 1117, Amsterdam, the Netherlands
[c] Amsterdam UMC, University of Amsterdam, Neurology and Clinical Neurophysiology, Amsterdam Neuroscience, Meibergdreef 9, Amsterdam, the Netherlands
[d] Amsterdam UMC, University of Amsterdam, Neurosurgery, Amsterdam Neuroscience, Meibergdreef 9, Amsterdam, the Netherlands

ARTICLE INFO

Keywords:
Parkinson's disease
Magnetoencephalography
Deep brain stimulation
Motor symptoms
Resting-state

ABSTRACT

Deep brain stimulation (DBS) of the subthalamic nucleus (STN) is an established symptomatic treatment in Parkinson's disease, yet its mechanism of action is not fully understood. Locally in the STN, stimulation lowers beta band power, in parallel with symptom relief. Therefore, beta band oscillations are sometimes referred to as "anti-kinetic". However, in recent studies functional interactions have been observed beyond the STN, which we hypothesized to reflect clinical effects of DBS.

Resting-state, whole-brain magnetoencephalography (MEG) recordings and assessments on motor function were obtained in 18 Parkinson's disease patients with bilateral STN-DBS, on and off stimulation. For each brain region, we estimated source-space spectral power and functional connectivity with the rest of the brain.

Stimulation led to an increase in average peak frequency and a suppression of absolute band power (delta to low-beta band) in the sensorimotor cortices. Significant changes (decreases and increases) in low-beta band functional connectivity were observed upon stimulation. Improvement in bradykinesia/rigidity was significantly related to increases in alpha2 and low-beta band functional connectivity (of sensorimotor regions, the cortex as a whole, and subcortical regions). By contrast, tremor improvement did not correlate with changes in functional connectivity.

Our results highlight the distributed effects of DBS on the resting-state brain and suggest that DBS-related improvements in rigidity and bradykinesia, but not tremor, may be mediated by an increase in alpha2 and low-beta functional connectivity. Beyond the local effects of DBS in and around the STN, functional connectivity changes in these frequency bands might therefore be considered as "pro-kinetic".

1. Introduction

Deep brain stimulation (DBS) of the subthalamic nucleus (STN) is an established and effective symptomatic treatment for the disabling medication-related response fluctuations in the motor symptoms of Parkinson's disease (Benabid et al., 2001; Deuschl et al., 2006). Tremor relief most likely involves different neuronal mechanisms than the reductions in bradykinesia and rigidity (Helmich, 2018; Louis et al., 1999). Local field potential (LFP) studies have demonstrated that excessive beta band synchronized oscillatory activity in the basal ganglia is a hallmark of Parkinson's disease and that DBS-induced suppression of these oscillations in the STN goes hand in hand with improvement of both bradykinesia and rigidity (Brown and Williams, 2005; Hammond et al., 2007; Kühn et al., 2006). Beta band oscillations have therefore been labelled as "anti-kinetic" ((Peter Brown, 2003), see also (McGregor and Nelson, 2019) for a recent discussion on this topic).

Recent observations suggest that DBS-related neurophysiological effects extend beyond the major components of the classical motor system (Abbasi et al., 2018; Airaksinen et al., 2012; Cao et al., 2015; Cao et al., 2017; Kahan et al., 2014; Luoma et al., 2018; Oswal et al., 2016) (for reviews on this topic see (Boon et al., 2019; Harmsen et al., 2018)). A better understanding of these effects is not only necessary to

* Corresponding author at: Amsterdam UMC, location VUmc, Neurology, Amsterdam Neuroscience, De Boelelaan 1117, Amsterdam, the Netherlands.
E-mail address: l.i.boon@amsterdamumc.nl (L.I. Boon).

https://doi.org/10.1016/j.nicl.2020.102225
Received 6 November 2019; Received in revised form 27 January 2020; Accepted 20 February 2020
Available online 21 February 2020

Abbreviations

AAL	automated anatomical labelling
cAEC	corrected amplitude envelope correlation
DBS	deep brain stimulation
FDR	false discovery rate
HPI	head position indicator
LEDD	levodopa equivalent daily dose
LFP	local field potential
MDS-UPDRS-III	Movement Disorders Society Unified Parkinson's Disease Rating Scale, motor part
MEG	magnetoencephalography
PLI	phase lag index
ROI	region of interest
SL	synchronization likelihood
SNR	signal-to-noise ratio
STN	subthalamic nucleus
tSSS	temporal extension of signal space separation

explain the neurophysiological mechanisms of DBS but might also aid in the development of an in-vivo biomarker for short and long-term therapeutic effects.

At the cortical level, STN-DBS can modulate oscillatory brain activity in several frequency bands. In two recent studies, STN-DBS lowered theta, alpha and low-beta band power in (Abbasi et al., 2018); source-space analysis) and over ((Luoma et al., 2018); sensor-space analysis) the sensorimotor cortex, but without a correlation with motor improvement (Abbasi et al., 2018; Luoma et al., 2018). Other studies demonstrated that an alpha and beta power suppression over right temporal brain regions correlated positively with DBS-related global motor improvement (Cao et al., 2017), whereas the average frequency of cortical oscillations seemed to increase upon stimulation (Airaksinen et al., 2012; Cao et al., 2015).

Neural circuits involved in Parkinson's disease symptoms can be subdivided into different parallel circuits that generally concern cortico-subcortical interactions (McGregor and Nelson, 2019; Nambu et al., 2002). STN-DBS might have opposing functional effects on these circuits as well as their elements. In an fMRI study, dynamic causal modelling revealed a reduction in effective connectivity of the hyperdirect pathway, whereas effective connectivity of the direct, cortico-striatal and thalamo-cortical pathways was increased upon stimulation (Kahan et al., 2014). Oswal and co-workers confirmed that stimulation of the STN suppressed upper-beta band coherence between the STN and cortical motor areas, possibly reflecting the hyperdirect pathway. However, these changes did not correlate with clinical improvement, whereas suppression of low-beta band power in the STN did (Oswal et al., 2016).

Using magnetoencephalography (MEG), Parkinson's disease related oscillatory activity can be studied with an excellent spatial and temporal resolution (Baillet, 2017; Oswal et al., 2016). MEG data can even be recorded successfully during DBS, in spite of the contamination of recordings by hardware and stimulation artefacts (see (Abbasi et al., 2016; Oswal et al., 2016) for a detailed description of DBS-related artefacts). To date, no studies have reported on the influence of DBS on whole-brain functional connectivity including cortico-subcortical connections. Here we investigated this influence using MEG in order to study the alleged anti-kinetic nature of beta band oscillations and to elucidate the neurophysiological correlates of DBS motor-effects.

We used the Amplitude Envelope Correlation (AEC; the correlation between the temporal evolution of spectral power in different regions) as a measure of functional connectivity (Brookes et al., 2012). The AEC is dissociated from local oscillatory processes, and therefore complementary to band power analysis (Hipp et al., 2012). In addition, the AEC has shown similarities with fMRI connectivity (Brookes et al., 2011), thereby allowing a direct comparison with fMRI data. Spurious correlations can be accounted for by using an orthogonalisation method (Colclough et al., 2015; Hipp et al., 2012).

In line with previous whole-brain studies (Airaksinen et al., 2012; Cao et al., 2015; Cao et al., 2017; Hill et al., 2013; Kahan et al., 2014), we expected the DBS-effects to extend beyond the 'classical' motor system. In addition, since DBS has been shown to influence oscillations in the alpha and low-beta band (Abbasi et al., 2018; Luoma et al., 2018) and functional connectivity in the low and high-beta band (Oswal et al., 2016), we hypothesized that alpha and beta band functional connectivity changes would reflect symptom relief upon DBS in Parkinson's disease. We therefore performed resting-state MEG recordings with and without STN-DBS stimulation, at least six months after DBS electrode placement. In addition, we assessed whether functional connectivity changes correlated with improvement in motor function, measured using the motor part of the Unified Parkinson's Disease Rating Scale (MDS-UPDRS-III).

2. Materials and methods

2.1. Patients

Parkinson's disease patients who had undergone bilateral implantation of STN DBS electrodes between 2016 and 2018 at Amsterdam UMC, location AMC, were included in this study. Eligibility for STN DBS placement has been described previously (Contarino et al., 2014). In the context of standard clinical care, the active contacts, voltage, pulse width and frequency of stimulation were individually determined for optimal therapeutic efficacy. Inclusion criteria for the study were: bilateral Boston Scientific Vercise Directed (Valencia, CA, USA) stimulation system (as pilot results demonstrated that this stimulation system was most compatible with our MEG system with respect to the head position estimation; when using a Medtronic Activa PC system (Minneapolis, Minnesota, USA) the noise introduced by the stimulator was such that the head position indicator coils could not be localised by the MEG system), DBS placement at least six months before the MEG recordings, and monopolar stimulation. Exclusion criteria were treatment with levodopa continuous intestinal gel or subcutaneous apomorphine, and permanent post-operative structural damage following DBS electrode placement that could affect the MEG results (apart from the DBS-placement itself).

Disease duration was calculated on the basis of the patients' estimation of the onset of the classical Parkinson's disease motor symptoms. The total dose of dopamine replacement therapy was converted to the levodopa equivalent daily dose (LEDD), as described previously (Olde Dubbelink et al., 2013). The research protocol was approved by the medical ethical committee of the Amsterdam UMC, location VUmc. Ethics review criteria conformed to the Helsinki declaration. After careful explanation of the procedures, all patients gave written informed consent.

2.2. Data acquisition

MEG data were recorded using a 306-channel whole-head system (Elekta Neuromag Oy, Helsinki, Finland) in an eyes-closed resting-state condition, with a sample rate of 1250 Hz, and online anti-aliasing (410 Hz) and high-pass (0.1 Hz) filters. Anatomical T1-weighted images of the head were obtained using a 3T MRI scanner (Philips Ingenia, Best, the Netherlands) in the context of standard clinical care before DBS placement. The study visit took place after an overnight withdrawal of dopaminergic medication (practically defined OFF state). The head position relative to the MEG sensors was recorded continuously using the signals from five head position indicator (HPI) coils. The HPI

positions were digitized before each recording, as well as the outline of the patient's scalp (~500 points), using a 3D digitizer (Fastrak, Polhemus, Colchester, VT, USA). For each patient total MEG recording time was 55 min, consisting of 11 trials of 5 min each in which different stimulation settings were explored. At the beginning of each individual trial, localization of the HPI coils was performed in the DBS OFF condition, following which one of the researchers, who monitored the patient inside the magnetically shielded room, changed the DBS-settings and recordings were started. During the recordings, the programming device was kept (offline) in the magnetically shielded room on a stable underground, at approximately 2.5 m distance from the MEG helmet. The experimental setup can be appreciated from Fig. 1.

The first recording was during stimulation with the standard (optimal) DBS settings of the individual patient (DBS ON). Then, nine recordings took place in randomized order, eight of which were during unilateral stimulation of one of the eight individual contact points (data not shown), and one recording during DBS OFF. The last recording was, again, during stimulation with the standard DBS settings of each individual patient (DBS ON2; data analysed as supplementary analysis). The time between recordings, including change of DBS settings and localization of the HPI coils, was at least 2 min.

MDS-UPDRS-III scores were measured during DBS ON and OFF on a separate day by trained nurses, approximately six months after DBS-placement. In accordance with the MEG-recordings, these scores were obtained in the dopamine OFF-state.

2.3. Data pre-processing

MEG channels that were malfunctioning, for example due to excessive noise, were removed after visual inspection of the data. Thereafter, the temporal extension of Signal Space Separation (tSSS; (Taulu and Hari, 2009; Taulu and Simola, 2006)) in MaxFilter software (Elekta Neuromag Oy, version 2.2.15) was applied with a sliding window of 10 s, origin (0,0,40), and harmonic expansions of 8 respectively 3 for the internal and external signals (all default settings), as well as subspace correlation-limit of 0.8 to suppress the strong magnetic artefacts, which has previously been demonstrated to result in satisfactory data quality without suppression of brain signals (Boring et al., 2019; Carrette et al., 2011; Medvedovsky et al., 2009; Taulu and Hari, 2009). An example of the effect of tSSS on MEG data recorded in our study is depicted in Supplementary Fig. 1. Patient's MEG data were co-registered to their structural MRIs using a surface-matching procedure, with an estimated resulting accuracy of 4 mm (Whalen et al., 2008). A single sphere was fitted to the outline of the scalp as obtained from the co-registered MRI, which was used as a volume conductor model for the beamformer approach described below.

The automated anatomical labelling (AAL) atlas was used to label the voxels in 78 cortical and 12 subcortical regions of interest (ROIs) (Gong et al., 2009; Tzourio-Mazoyer et al., 2002). We used each ROI's most central voxel (centroid) as the representative for that ROI (Hillebrand et al., 2016b). Subsequently, an atlas-based beamformer approach was used to project broad-band (0.5–48 Hz) filtered sensor signals to these centroid voxels (Hillebrand et al., 2012), resulting in broad-band time-series for each centroid of the 90 ROIs. MEG data were visually inspected (by LIB) for tremor-, motion- and stimulation-related artefacts and drowsiness. In addition, for each recording, the 50% epochs with the slowest peak frequency were discarded in order to make the occurrence of drowsiness in the selected data even more unlikely. Epochs contained 4096 samples (3.28 s), and for each condition, 20 epochs with the best quality recordings were selected for further analysis. Spectral and functional connectivity analyses were performed using in-house software (BrainWave, version 0.9.152.12.26; CJS, available from https://home.kpn.nl/stam7883/brainwave.html). For frequency band specific analyses, epochs were filtered in six frequency bands (delta (0.5–4 Hz), theta (4–8 Hz), alpha1 (8–10 Hz), alpha2 (10–13 Hz; as the distinction between alpha1 and alpha2 oscillations does have functional significance (Klimesch et al., 2005)), low-beta (13–22 Hz) and high-beta (22–30 Hz), using a fast Fourier Transform.

2.4. Data analysis

We estimated the overall absolute spectral power (0.5–48 Hz) averaged over all ROIs and normalised based on the maximum power peak (Fig. 2), as well as the absolute spectral power for each frequency band and ROI separately (Fig. 3). Peak frequency values were estimated within the 4–13 Hz frequency range.

For each epoch, frequency-band specific functional connectivity was estimated using the corrected cAEC, an implementation of the AEC (Brookes et al., 2012) corrected for volume conduction/field spread, using a symmetric orthogonalisation procedure (Brookes et al., 2012; Hipp et al., 2012). The cAEC was calculated for all possible pairs of ROIs, leading to a 90×90 adjacency matrix that contained the functional connectivity values between all ROI pairs.

2.5. Statistical analysis

For each patient, stimulation condition and frequency band separately, absolute power and cAEC matrices were averaged over 20 epochs. Both mean absolute power and mean cAEC per ROI, hence, functional connectivity of one ROI with the rest of the brain, were compared between the ON and OFF stimulation condition using permutation tests (Maris and Oostenveld, 2007; Nichols and Holmes, 2002) ($N = 10{,}000$; $p < 0.05$). Correction for false positives

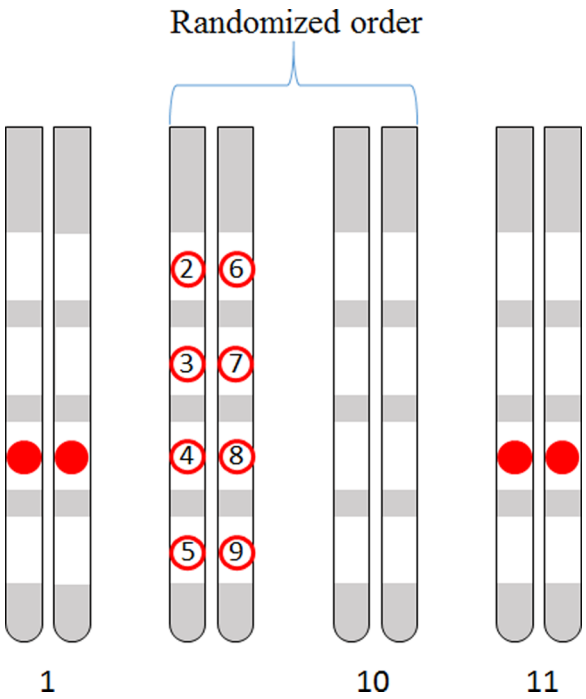

Fig. 1. Experimental setup.
Overview of the different DBS settings during the MEG recordings. The bilateral electrodes, each having four contact points are depicted (the two middle contact points consisted of triplets of segments, together used as one contact point). During the first MEG recording (1) both electrodes were stimulated in the optimal settings of the patient. The second to tenth MEG recordings took place in a randomized order, during which each of the eight individual contact points were stimulated once (2 & 6, dorsal; 3 & 7, dorsomedial; 4 & 8, ventromedial; 5 & 9 ventral; outside the scope of this study), and one recording took place during DBS OFF (10). During the last MEG recording, both electrodes were, again, stimulated in the optimal settings of the patient (11).

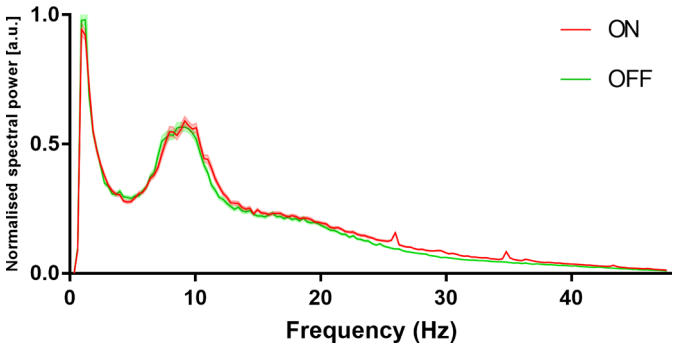

Fig. 2. Overall power spectrum. Average of normalised frequency spectra for all patients ($n = 18$) and all regions of interest ($n = 90$), shaded areas indicate standard error of the means. Despite tSSS filtering and the beamforming approach, stimulation artefact peaks remained present at 27 Hz and 35 Hz during DBS ON (red). DBS, deep brain stimulation; tSSS, spatiotemporal Signal Space Separation. (For interpretation of the references to color in this figure legend, the reader is referred to the web version of this article.)

was performed using the 'false discovery rate' (FDR), separately for each frequency band, with a p-value for each of the 90 ROIs as input (Benjamini and Hochberg, 1995).

The correlations between DBS-related improvement in motor function and changes in functional connectivity were estimated using Spearman tests (without correction for multiple comparisons due to the exploratory nature of the analysis), where percentage improvement in total MDS-UPDRS-III, bradykinesia/rigidity (items 3–7) and tremor (items 15–18) scores were used as measures of motor improvement. Functional connectivity changes were obtained for all six frequency bands averaged over ROIs in i) the sensorimotor cortices (bilateral pre and post-central gyri), ii) all cortical regions, and iii) all subcortical regions. Only patients who had tremor during DBS OFF were selected for correlation analyses on tremor improvement.

2.6. Data availability statement

The data and codes used in this study are available from the corresponding author, upon reasonable request.

3. Results

3.1. Patients

Twenty-one Parkinson's disease patients participated in this study and underwent MEG recordings at Amsterdam UMC, location VUmc, at least 6 months after DBS placement (range 6–15 months). Three patients were excluded from further analysis since their MEG data had too many dysfunctional channels during stimulation (>~13 channels, caused by excessive noise), which prevented the use of tSSS. This led to a final group of 18 Parkinson's disease patients treated with DBS (mean age 58.4 y, SD 8.3), whose characteristics are summarized in Table 1. Thirteen patients suffered from tremor and were used for correlations between functional connectivity changes and tremor effects of DBS (paragraph 3.4). The mean number of excluded MEG channels was 9 for DBS ON recordings (range: 5–13) and 6 for DBS OFF recordings (range: 2–12).

3.2. Spectral power

Fig. 2 shows global stimulation-related normalized spectral power for all Parkinson's disease patients. The peak frequency was significantly (and, for all but one patient, consistently) higher during stimulation ON compared to stimulation OFF (DBS ON 8.79 Hz ± 0.69; DBS OFF 8.54 ± 0.64 Hz; $t(17) = 5.16$; $p < 0.001$). Two stimulation-related spectral peaks were not removed by tSSS and beamforming. For all patients, these peaks were present around 27 Hz and 35 Hz. Fig. 3 displays significant differences in absolute power per frequency band between DBS ON and DBS OFF. During DBS ON, a decrease in (mostly occipital) power was observed in the delta and theta band, and an increase in band power was observed in the alpha2, low-beta and high-beta band. This suggests a spectral shift towards the higher frequencies. The sensorimotor cortices were hardly involved in this shift, and even showed a right-sided suppression of band power in the frequency range between 0.5 and 22 Hz.

3.3. Functional connectivity

To assess differences in average functional connectivity *per ROI* between DBS ON and DBS OFF, permutation tests were performed for

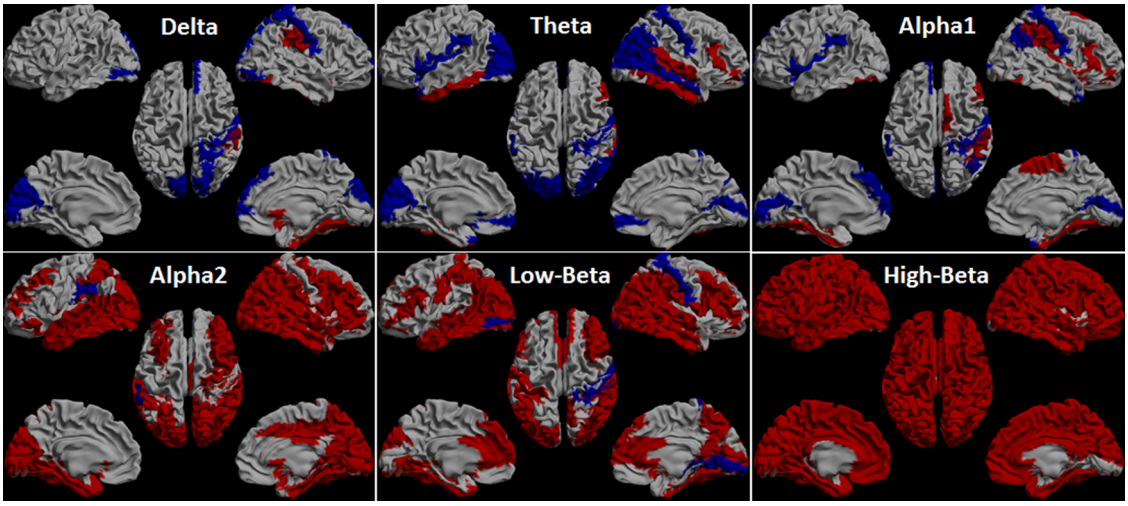

Fig. 3. Regional band power changes. Distribution of significant differences ($p < 0.05$, FDR corrected) in absolute band power between DBS ON and DBS OFF. Significant increases (decreases) are displayed in red (blue) on a parcellated template brain viewed from, in clockwise order, the left, top, right, left-midline and right-midline. For visualisation purposes, only cortical brain regions are displayed. During DBS ON, a decrease in (mostly occipital) power was observed in the delta and theta band, and an increase in band power was observed in the alpha2, low-beta and high-beta band, suggesting a spectral shift towards the higher frequencies during DBS ON. Note that the sensorimotor regions were hardly involved in this shift and, instead, showed a decrease in absolute band power for the delta, theta, alpha1, alpha2 and low-beta band.

Table 1
Patient characteristics.

Patient	Age (years)	Sex	Disease duration (years)	Stimulation parameters (stimulation side; contact point on electrode; intensity (mA))	Pulse width and stimulation frequency	Levodopa equivalent dose (mg/day)		Motor MDS-UPDRS (III)				Tremor subscore (MDS-UPDRS (III))	
						Pre-DBS	Post-DBS	Med OFF/ pre-DBS	Med OFF	OFF/DBS	Med OFF/DBS ON	Med OFF/ DBS OFF	Med OFF/ DBS ON
1	38	M	8	L; DM; 2.9 R; VM; 3.4	60 μs 179 Hz	1644	996	73	54	31	9		4
2	63	F	5	L; DM; 1.7 R; DM; 1.7	60 μs 130 Hz	495	567	43	16	11	0		0
3	65	F	27	L; VM; 2.7 R; DM; 1.5	60 μs 130 Hz	500	400	33	20	19	4		3
4	49	F	10	L; D; 1.9 R; D; 2.5	60 μs 130 Hz	797	536	35	37	22	1		0
5	69	M	12	L; DM; 2.1 R; DM; 2.1	60 μs 130 Hz	1830	150	56	24	14	2		0
6	60	M	8	L; DM; 3.2 R; DM; 1.3	60 μs 179 Hz	1200	300	57	65	38	8		0
7	53	M	11	L; DM; 2.9 R; DM; 1.9	60 μs 130 Hz	1567	1043	60	44	30	4		3
8	66	F	8	L; VM; 2.2 R; DM; 1.8	60 μs 130 Hz	1226	753	47	37	33	11		6
9	45	M	5	L; D; 1.7 R; DM; 1.7	60 μs 130 Hz	1410	283	50	80	44	12		2
10	70	F	25	L; DM; 2.1 R; DM; 2.4	60 μs 130 Hz	1590	555	46	33	15	0		0
11	66	M	10	L; DM; 2.5 R; DM; 1.8	60 μs 149 Hz	750	575	38	54	27	7		3
12	55	M	8	L; DM; 2.7 R; DM; 2.6	60 μs 130 Hz	950	775	42	31	15	0		0
13	57	M	11	L; VM; 1.6 R; VM; 1.6	60 μs 130 Hz	1134	606	38	21	7	0		0
14	61	M	7	L; VM; 1.5 R; VM; 2.1	60 μs 130 Hz	1000	375	30	27	11	2		0
15	60	M	14	L; DM; 2.0 R; VM; 2.5	60 μs 130 Hz	1073	425	55	27	7	3		1
16	57	M	12	L; VM; 3.1 R; VM; 2.3	60 μs 130 Hz	1380	720	80	52	26	5		3
17	61	M	8	L; DM; 1.8 R; DM; 2.3	60 μs 130 Hz	1726	946	56	52	21	8		1
18	56	M	12	L; DM; 1.4 R; VM; 1.3	60 μs 130 Hz	2131	1245	45	20	10	0		0
Mean (SD)	58 (8)	M, $n = 13$; F, $n = 5$	11 (6)	L: 2.2 (0.54) R: 2.0 (0.52)		1245 (456)	625 (294)	49 (13)	39 (18)	21 (11)	4 (4)		1 (2)

mA, milliampere; μs, microseconds; LEDD, Levodopa Equivalent Daily Dose; MDS-UPDRS-III, Movement Disorders Society Unified Parkinson's Disease Rating Scale motor ratings; DBS, Deep Brain Stimulation; M/F, male/female; L/R, left/right; D/DM/VM, Dorsal/Dorsomedial/Ventromedial; Med, medication.

Table 2
Significant differences in average cAEC values per region of interest.

Frequency band	Anatomical region	L/R	cAEC (DBS ON)	cAEC (DBS OFF)	↑ or ↓	*P*-value (FDR-corrected)
Alpha2	Middle temporal gyrus	L	0.504	0.499	↑	0.0090
	Gyrus rectus	L	0.514	0.511	↑	0.0210
	Olfactory cortex	L	0.515	0.512	↑	0.0210
	Superior frontal gyrus, orbital part	L	0.513	0.510	↑	0.0210
	Inferior frontal gyrus, triangular part	L	0.511	0.515	↓	0.0210
	Superior frontal gyrus	L	0.510	0.514	↓	0.0090
Low-beta	Superior parietal gyrus	L	0.509	0.513	↓	0.0090
	Anterior cingulate gyrus	L	0.511	0.514	↓	0.0461
	Gyrus rectus	R	0.512	0.510	↑	0.0475
	Superior frontal gyrus, orbital part	R	0.511	0.509	↑	0.0399
	Superior temporal pole	R	0.510	0.512	↓	0.0475
	Thalamus	L	0.518	0.512	↑	0.0475

Comparison between the DBS ON state and the DBS OFF state. Significance threshold $p < 0.05$.
L, Left; R, Right; cAEC, corrected Amplitude Envelope Correlation; DBS, Deep Brain Stimulation; FDR, False Discovery Rate.

all 90 ROIs in the six frequency bands. Significant differences in cAEC were found for the low-beta band (ten ROIs) and also for the alpha2 band (one ROI) and are listed in Table 2 (as well as visualized in Supplementary Fig. 2). The regions that showed the largest increases in functional connectivity following stimulation were mainly located in bilateral frontobasal brain regions, whereas regions that showed significant decreases followed a more dispersed pattern (frontal, parietal and temporal lobes, bilaterally).

3.4. Relationship between clinical motor improvement and functional connectivity changes

A significant positive correlation was found between total DBS-related motor improvement (MDS-UPDRS-III) and low-beta cAEC change in the sensorimotor cortices ($r_{SM}(16) = 0.58$, $p = 0.011$), the whole cortex ($r_{WC}(16) = 0.50$, $p = 0.035$), and all subcortical regions ($r_{SC}(16) = 0.62$, $p = 0.006$) (Fig. 4). When only the MDS-UPDRS-III subscores for bradykinesia and rigidity were considered, the correlations with low-beta band cAEC change were even stronger (respectively: $r_{SM}(16) = 0.61$, $p = 0.007$; $r_{WC}(16) = 0.70$, $p = 0.001$; $r_{SC}(16) = 0.76$, $p < 0.001$) (Fig. 4). In addition, a significant positive correlation was found between bradykinesia/rigidity subscores and alpha2 band cAEC changes ($r_{SM}(16) = 0.57$, $p = 0.014$; $r_{WC}(16) = 0.72$, $p = 0.001$; $r_{SC}(16) = 0.68$, $p = 0.002$) (Supplementary Table 1). cAEC changes did not correlate significantly with tremor improvement (Fig. 4; Supplementary Table 1).

4. Discussion

In this study, we investigated stimulation effects of STN DBS on whole-brain functional connectivity in 18 Parkinson's disease patients. We found that increases in alpha2 and low-beta band functional connectivity were correlated with DBS-related improvements in bradykinesia and rigidity, but not with tremor relief. This suggests that the alleged *anti-kinetic* role of beta band oscillations (Hammond et al., 2007; Heinrichs-Graham et al., 2014; Levy et al., 2002; Silberstein et al., 2005) does not apply when large-scale cortico-cortical and cortico-subcortical functional interactions are taken into account. In addition, and in accordance with previous studies (Abbasi et al., 2018; Airaksinen et al., 2012; Luoma et al., 2018), we found a suppression of sensorimotor cortical oscillatory activity (ranging from delta to low-beta band) against a background of widespread stimulation-related increases in oscillatory brain activity involving the higher frequencies.

4.1. Band power

Our present observations confirm previous results on band power changes associated with DBS. Firstly, during DBS ON, throughout the cerebral cortex, higher absolute band powers were observed for the higher frequencies (10–30 Hz), whereas lower absolute band powers were found for the lower frequencies (0.5–8 Hz), which could be interpreted as an overall acceleration of oscillatory brain activity. Furthermore, during DBS ON the alpha peak frequency was significantly higher than during DBS OFF. However, since the DBS ON recording was always the first recording of the day, we cannot exclude the possibility that the order of recordings (for example due to increased drowsiness in subsequent recordings) added to the observed spectral shift. Therefore, we additionally studied spectral power in the ON2 recording, which always took place as the last recording. In Supplementary Fig. 3 we illustrate the band power differences between ON2 and DBS OFF ($n = 17$, data for one patient was excluded due to excessive noise of the ON2 recording): Again, stimulation led to an increase in band power for the higher frequencies (8–30 Hz), and a higher frequency of the alpha peak (DBS ON2 8.64, SD 0.69 vs DBS OFF 8.55, SD 0.65; $t(16) = 2.06$, $p = 0.056$). Hence, we conclude that the observed acceleration of oscillatory brain activity is stimulation related, which is in line with the results of an earlier study (Airaksinen et al., 2012)). This effect has previously been attributed to a non-specific increase in intrinsic alertness, independent of motor function (Fimm et al., 2009; Jech et al., 2006). Alternatively, it may reflect a stimulation-related "release" of the thalamus, which affects cortical brain rhythms (DeLong and Wichmann, 2007). However, we cannot exclude the possibility that noise from the stimulator changes the aperiodic "background" 1/f component of the neural power spectrum, thereby causing a peak frequency shift towards the faster frequencies (Haller et al., 2018). Secondly, we confirmed alpha and beta band suppression in the sensorimotor regions which was previously observed after DBS in Parkinson's disease patients (Abbasi et al., 2018; Luoma et al., 2018) and following transcranial direct current stimulation over the sensorimotor cortex in healthy controls (Pellegrino et al., 2018), although this effect was less distinct in our study. Perhaps the fact that our recordings took place in an eyes-closed condition, during which the posterior dominant alpha rhythm is stronger than during an eyes-open condition, may have "blurred" these specific effects.

4.2. Functional connectivity

The presently observed correlation between increases in functional connectivity and improvements in bradykinesia and rigidity scores is in contradiction with the observations reported by Silberstein and coworkers, who were the first (and up to now the only) to study the effect of DBS on whole-brain functional connectivity (Silberstein et al., 2005). They used coherence analysis of (scalp-recorded) EEG data, obtained in DBS-patients with and without stimulation and found reductions in 10–35 Hz coherence between EEG channels that correlated with overall MDS-UPDRS-III improvement. A potential explanation for the discrepancy with our results is the sensitivity of coherence analysis to

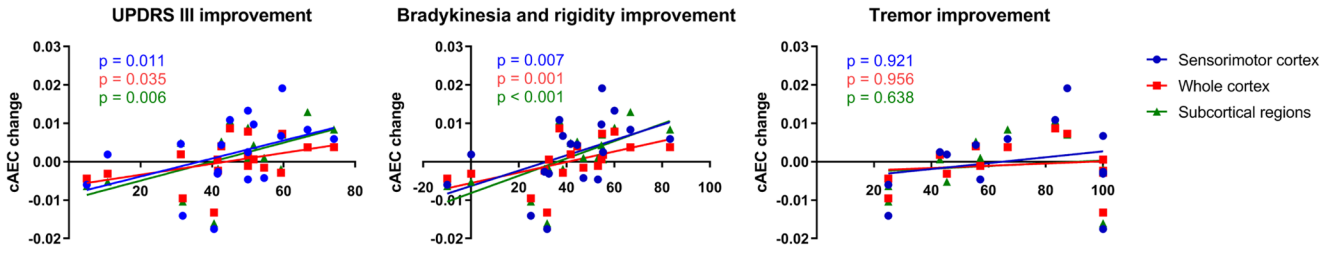

Fig. 4. Correlation of functional connectivity changes with improvement in motor scores. Scatter plots of clinical improvement values and low-beta functional connectivity changes (averaged for respectively the sensorimotor cortices, whole cortex and subcortical regions). Left: Significant correlations between MDS-UPDRS-III improvement (% comparing ON versus OFF-DBS) and cAEC changes (absolute difference ON versus OFF-DBS). Sensorimotor cortices ($r_{SM}(16) = 0.58$, $p = 0.011$), whole cortex ($r_{WC}(16) = 0.50$, $p = 0.035$), and all subcortical regions ($r_{SC}(16) = 0.62$, $p = 0.006$). Middle: Significant correlations between bradykinesia/rigidity improvement and cAEC changes ($r_{SM}(16) = 0.61$, $p = 0.007$; $r_{WC}(16) = 0.70$, $p = 0.001$; $r_{SC}(16) = 0.76$, $p < 0.001$). Right: Tremor improvement ($n = 13$ patients) and cAEC change, no significant correlation. All correlations tested can be found in Supplementary Table 1. cAEC, corrected Amplitude Envelope Correlation; MDS-UPDRS-III, Movement Disorders Society Unified Parkinson's Disease Rating Scale motor ratings.

volume conduction and band power changes (and thereby signal-to-noise ratio (SNR) changes) (Palva and Palva, 2012; Schoffelen and Gross, 2009). Indeed, the authors observed positive correlations between therapy-induced power and coherence changes. Hence, taking into account the reduction of (mostly alpha and beta band) power around the sensorimotor cortex due to DBS (Abbasi et al., 2018; Luoma et al., 2018), the correlations between reduced coherence and improvement of motor function reported by Silberstein et al. may have been influenced by band power changes. In addition, although unlikely to be the sole explanation for the discrepancy between the two studies, MEG and EEG measure different components of the electromagnetic fields generated by neuronal activity, resulting in different sensitivity profiles (Goldenholz et al., 2009; Muthuraman et al., 2014). Importantly, although cortico-subcortical functional connections do seem to matter (Supplementary Fig. 4C), the correlations we observed between increases in functional connectivity and clinical improvement cannot fully be explained by the inclusion of subcortical brain regions in our study, since this correlation remained after excluding cortico-subcortical interactions from our analyses (results not shown).

So far, two MEG-studies have assessed the influence of an acute dopaminergic challenge on whole-brain functional connectivity. Stoffers et al. demonstrated, upon levodopa administration, increases in both short-distance functional connectivity (averaging connectivity values for all possible sensor pairs overlying a lobe; 4–30 Hz) and long-range functional connectivity (averaging values for all possible sensor pairs between two lobes; 13–30 Hz), assessed using the synchronization likelihood (SL). In patients with a strong dopamine-related improvement in motor scores, motor improvement was associated with *decreases* in local beta band SL (Stoffers et al., 2008). Although we have confirmed the range of effects of DBS on functional connectivity in this study, i.e. both decreases and increases, strongest bradykinesia and rigidity improvement were related to *increases* in functional connectivity in our study. Again, volume conduction might have played a role in this partial discrepancy, since SL is sensitive to volume conduction/field spread and the functional connectivity analysis was performed in sensor space. Volume conduction/field spread leads to multiple recording sites picking up signals from a single source, which may result in erroneous estimates of functional connectivity (Schoffelen and Gross, 2009). The fact that only *local* beta band SL showed the discrepancy described supports the notion that volume conduction/field spread might have affected the relationship that was found. In accordance with this line of reasoning, using a functional connectivity measure that is insensitive to the effects of volume conduction/field spread (phase lag index; PLI) others have also found a positive correlation between functional connectivity changes in the left parietal area and improvement in motor function after a dopamine challenge (Cao et al., 2018).

In contrast with the aforementioned studies, our main results are not based on an acute DBS stimulation challenge, but rather compares DBS ON with DBS OFF. We did however record acute stimulation data in the optimal settings of the patient at the end of each experiment, namely during condition DBS ON2. Although this recording started immediately after switching on the DBS and stimulation effects may not have been maximally present yet, we again found a significant correlation between functional connectivity increases in the subcortical regions and bradykinesia/rigidity improvement (r_{SC} *(15)* = 0.57, p = 0.017), as well as positive trends for the sensorimotor regions (r_{SM} *(15)* = 0.43, p = 0.088) and the cortex as a whole (r_{WC} *(15)* = 0.36, p = 0.152). Therefore, we conclude that the order of stimulation (first DBS ON recording and then the DBS OFF recording, or the other way around) has not influenced the observed direction of correlations found.

In the present study, a differential effect of DBS on alpha2 and low-beta functional connectivity was found. As shown in Supplementary Fig. 4, in Parkinson's disease patients who had a modest clinical response to DBS we observed a decrease in whole-brain functional connectivity, whereas in Parkinson's disease patients who had a good clinical response we observed an increase, involving cortico-subcortical connections (Supplementary Fig. 4C). We propose the possibility of a technical as well as a physiological explanation for the observed effect.

The technical explanation involves the potential effect of stimulation artefacts in the DBS ON condition, and thereby the addition of 'noise', onto the reconstructed neuronal signals. The effect of the resulting changes in SNR on source level functional connectivity is complex, but stimulation-related noise may have had a lowering effect on functional connectivity (see Schoffelen and Gross, 2009) for further reading). Along this line of reasoning, stimulation could have led to a lowering in global functional connectivity for *all* DBS-patients, on top of which small increases in functional connectivity co-occurred with slight clinical improvement (but were covered by noise-related functional connectivity decreases) and large increases in functional connectivity co-occurred with strong clinical improvement (which became apparent as functional connectivity increases). In Supplementary Fig. 5 we show that the addition of spatially correlated white noise onto brain signals of two of our DBS-patients during DBS OFF indeed leads to a global decrease in estimated low-beta cAEC. This illustrates that the extra noise introduced by deep brain stimulation (simulated here as spatially correlated white noise) could have led to a reduction in estimated functional connectivity values. However, the addition of spatially correlated white noise hardly affected theta cAEC values in one patient. Hence, this effect seems frequency-dependent, and is perhaps related to the more prominent presence of amplitude envelope correlations in the alpha and beta band (Hipp et al., 2012).

An alternative, physiological, explanation for the observed differential effect may lie in the complex balance between the different cortico-subcortical functional circuits that converge in the STN. Stimulation in and around the STN can affect cortical brain regions antidromically via axonal stimulation, and can also have downstream effects on the cortico-striato-thalamic loop. We hypothesize that a shift in balance from antidromic axonal towards downstream activation effects might play a role in the link between better clinical effects and increases in functional connectivity. An overview of the hypothesis can be found in Fig. 5 and reads as follows:

Antidromic stimulation effects of axons (en route to other structures, or of axons that terminate in the STN) can affect the motor cortex via the hyperdirect pathway, but can also affect a wide variety of other cortical brain regions (Accolla et al., 2016; Whitmer et al., 2012). Stimulation effects downstream from the stimulated STN affect the cortico-striato-thalamic loop. The net effect on functional connectivity might not be the same for antidromic axonal and downstream stimulation effects. A dynamic causal modelling study demonstrated that upon DBS, the effective functional connectivity strength of the hyperdirect and indirect (striato-STN and STN-thalamus) pathway decreased, whereas the strength of the direct cortico-striato-pallido-thalamic pathway increased (Kahan et al., 2014), the latter being suggested by an empirical fMRI study (Mueller et al., 2018), as well as by our own additional visualizations in patients with a good clinical response, who had increases in cortico-subcortical functional connectivity (Supplementary Fig. 4C; although we lack the spatial resolution to draw conclusions on the functional connectivity profiles of individual subcortical brain regions). Via downstream activation effective modulation of the STN could reduce the indirect inhibitory drive from the subthalamic nucleus to the thalamus, which would "release" the thalamus to communicate with cortical brain regions (DeLong and Wichmann, 2007; Nambu et al., 2002). Furthermore, beneficial effects of stimulation on the resting motor system were better explained by strengthening the coupling along the direct pathway, and not by reducing coupling along the hyperdirect pathway (Kahan et al., 2014; Nambu et al., 2002). This observation was supported by an MEG study by Oswal et al., who found that a stimulation-related decrease in functional connectivity of the hyperdirect pathway was not related to clinical improvement (Oswal et al., 2016).

We expect the individual anatomy of white matter tracts, as well as the exact stimulation site in and around the STN (illustrated in

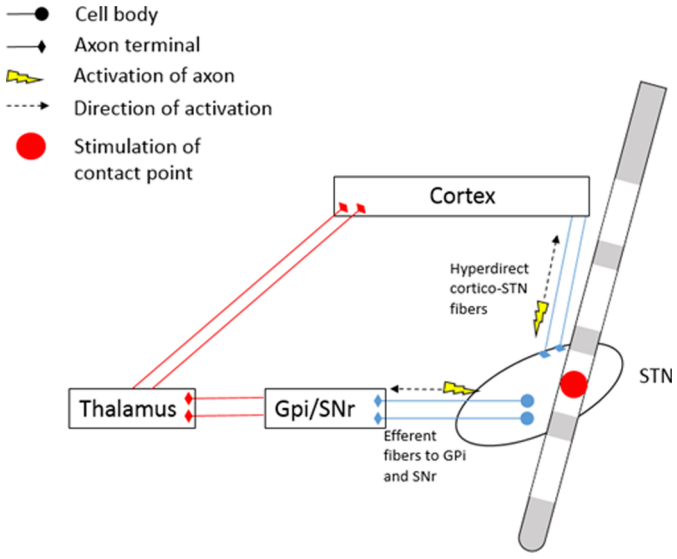

Fig. 5. Model of antidromic and downstream activation in STN-DBS. Stimulation effects in the antidromic direction take place upon stimulation of axons of the hyperdirect pathway. These stimulation effects may cause a suppression of band power in frontal cortical brain regions, as well as a lowering of functional connectivity between the frontal cortex and the STN (in blue; see also (Abbasi et al., 2018; Luoma et al., 2018; Oswal et al., 2016)). At the same time, stimulation effects can propagate in the downstream direction and thereby mainly affect the cortico-striato-thalamic loop. Downstream stimulation effects may lead to an increase in cortical functional connectivity via disinhibition of the thalamus (in red; (Mueller et al., 2018; Nambu et al., 2002)). Gpi, internal globus pallidus; SNr, substantia nigra pars reticulate; STN, subthalamic nucleus; DBS, deep brain stimulation. (For interpretation of the references to color in this figure legend, the reader is referred to the web version of this article.)

Supplementary Fig. 6 and Supplementary Table 2), to play a crucial role in the balance between antidromic axonal and downstream activation effects. Clearly, our hypothesis will have to be substantiated in future studies that combine local stimulation effects with whole-brain effects, such as LFP recordings combined with MEG recordings. In addition, the MEG data recorded in our study during stimulation of each individual contact point (data not shown), will be analysed in future studies and may shed further light on this matter.

4.3. Methodological issues

Several methodological issues deserve consideration. (i) In our study, DBS was off for several minutes before we started the 5 min recording. We expect that stronger DBS-related effects could have been observed if the period between turning off the DBS and the start of the MEG-recording had been longer. During epoch selection, we prioritized epochs from later parts of the recordings. However, considering that at least 50% of the total clinical change seems to occur within 5 min after the DBS is turned off (Little et al., 2013), and since we did observe significant changes in brain activity in parallel with a clinical correlate, we believe that our experimental setup was effective. (ii) The MDS-UPDRS-III assessments were always performed 6 months after DBS-placement, whereas the MEG recordings took place between six and fifteen months after surgery. The six months' time period made sure that the patients were measured in a clinically stable state. In one patient the stimulation was switched to a more dorsal contact point in the period between clinical assessments and the MEG recordings, due to non-motor side effects (patient 4). In all other patients, clinical assessments and MEG recordings took place during stimulation of the same contact points and with approximately the same stimulation strength (mean difference left-sided contact points 0.12 mA SD 0.25; right-sided contact points 0.05 mA SD 0.21). Although this separation in time may have affected our results, the correlation between clinical improvement and functional connectivity changes would probably have been even stronger if the MEG recordings and clinical assessments had taken place on the same day.

(iii) The use of the temporal extension of tSSS (Taulu and Hari, 2009; Taulu and Simola, 2006) allowed us to study brain signals during DBS. Despite the ability of tSSS and beamforming to effectively suppress artefacts ((Hillebrand et al., 2013); see also Supplementary Fig. 7 for the effect of tSSS on magnetometers and gradiometers separately), two sharp stimulation-related peaks were seen in the power spectrum (Fig. 1), in line with previous research (Airaksinen et al., 2012). We are aware that monopolar stimulation is associated with stronger artefacts than bipolar stimulation, but we chose to stimulate in the monopolar setting in our study as this represented the clinical setting of our patients. The peaks appeared not to affect the frequency range below 22 Hz, which encouraged us to separately consider the low-beta band and the high-beta band, and to refrain from analysing the gamma band. The observed relationship between alpha2 and low-beta functional connectivity changes and clinical improvement seem to confirm the validity of our recording and analysis approach. Obviously, the high-beta band results should be interpreted with caution and the stimulation-related increase in high-beta band power (Fig. 3) may be related to a stimulation artefact; In addition, the lack of a clinical correlate with high-beta band functional connectivity could also mean that stimulation artefacts affected the reconstruction of the brain signals too much in this band or, alternatively, that high-beta band functional connectivity does not reflect DBS-related clinical improvement. (iv) Methodological advances in beamforming (Hillebrand and Barnes, 2005; Hillebrand et al., 2005) allow MEG signals to be projected onto an atlas-based source space encompassing both cortical and subcortical brain regions (Boon et al., 2017; Hillebrand et al., 2016a). In the present study, this approach enabled us to study large scale cortico-subcortical interactions six months after surgery when 'stun effects' of the DBS placement have disappeared, instead of directly after surgery using LFP analysis with externalised DBS leads. Previous LFP studies have analysed fine-grained interactions between the STN and the cortex (e.g. (Hirschmann et al., 2013; Hirschmann et al., 2011, Litvak et al., 2011; Oswal et al., 2016), whereas our study lacks this spatial resolution. We were therefore not able to draw conclusions regarding individual subcortical regions, yet our coarser approach is complementary to the existing literature. (v) The lack of a correlation between functional connectivity changes and tremor improvement may reflect a difference in pathophysiological mechanisms underlying bradykinesia/rigidity on the one hand and tremor on the other hand. However, we cannot exclude the possibility of a false-negative finding, since the number of patients suffering from tremor was lower than the number of patients suffering from bradykinesia/rigidity ($n = 13$ versus $n = 18$, respectively). In addition, the lack of correlation may be driven by the patients with 100% tremor improvement, who demonstrated an unexpected lowering of functional connectivity upon stimulation (considering the results for patients with less improvement). However, we do not have a plausible explanation for this observation. (vi) Lastly, the correlations between clinical improvement and functional connectivity changes might have been affected by the stimulation strength or the dopaminergic state of the patients. However, we did not correct for this, since these parameters did not correlate with clinical improvement (correlation LEDD and bradykinesia/rigidity improvement $r(16) = 0.340$, $p = 0.168$; correlation stimulation strength and bradykinesia/rigidity improvement $r(16) = 0.012$, $p = 0.961$).

4.4. Conclusion

In conclusion, we found a DBS-related suppression of sensorimotor cortical oscillatory activity against a background of widespread stimulation-related increases in oscillatory brain activity involving the

higher frequencies. Increases in alpha2 and low-beta functional connectivity were correlated with bradykinesia/rigidity improvement, but not with tremor improvement. Our results provide new insights in the mechanism of action of DBS as they complement the alleged “anti-kinetic” effect of beta band oscillations, and suggest a “pro-kinetic” effect when large-scale cortico-cortical and cortico-subcortical functional interactions are taken into consideration.

Funding

This work was supported by Amsterdam Neurocience 05 Amsterdam Neuroscience Alliance Project - ND2016, which had no role in the study design, in collection/analysis/interpretation of the data, in writing of the report, and in the decision to submit the article for publication.

Declaration of Competing Interests

The authors report no competing interests.

Acknowledgements

We would like to thank all patients for their participation. We thank Gosia Iwan, Miranda Postma, Marije Scholten, Rosanne Prins, and Sharon Stoker-van Dijk for the MDS-UPDRS-III assessments, as well as their help with patient inclusions. We also thank Karin Plugge, Nico Akemann and Marieke Alting Siberg for the MEG acquisitions, and Pelle Wilbers for help with pre-processing and preliminary analyses.

Supplementary materials

Supplementary material associated with this article can be found, in the online version, at doi:10.1016/j.nicl.2020.102225.

References

Abbasi, O., Hirschmann, J., Schmitz, G., Schnitzler, A., Butz, M., 2016. Rejecting deep brain stimulation artefacts from MEG data using ICA and mutual information. J Neurosci Methods 268, 131– 141 . https://doi.org/10.1016/j.jneumeth.2016.04.010 .

Abbasi, O., Hirschmann, J., Storzer, L., Ozkurt, T.E., Elben, S., Vesper, J., Butz, M., 2018. Unilateral deep brain stimulation suppresses alpha and beta oscillations in sensorimotor cortices. Neuroimage 174, 201– 207 . https://doi.org/10.1016/j.neuroimage.2018.03.026 .

Accolla, E.A., Herrojo Ruiz, M., Horn, A., Schneider, G.H., Schmitz-Hubsch, T., Draganski, B., Kuhn, A.A., 2016. Brain networks modulated by subthalamic nucleus deep brain stimulation. Brain 139 (Pt 9), 2503– 2515 . https://doi.org/10.1093/brain/aww182 .

Airaksinen, K., Butorina, A., Pekkonen, E., Nurminen, J., Taulu, S., Ahonen, A., Makela, J.P., 2012. Somatomotor mu rhythm amplitude correlates with rigidity during deep brain stimulation in Parkinsonian patients. Clin Neurophysiol 123 (10), 2010– 2017. Retrieved from http://www.ncbi.nlm.nih.gov/pubmed/22513261 S1388-2457(12)00229-5 [pii];10.1016/j.clinph.2012.03.004 [doi] .

Baillet, S., 2017. Magnetoencephalography for brain electrophysiology and imaging. Nat. Neurosci. 20 (3), 327– 339 .

Benabid, A.L., Koudsie, A., Benazzouz, A., Vercueil, L., Fraix, V., Chabardes, S., Pollak, P., 2001. Deep brain stimulation of the corpus luysi (subthalamic nucleus) and other targets in Parkinson's disease. Extension to new indications such as dystonia and epilepsy. J. Neurol. 248 (3) SupplIii37-47 .

Benjamini, Y., Hochberg, Y., 1995. Controlling the false discovery rate: a practical and powerful approach to multiple testing. J. R. Stat. Soc. Ser. B (Methodological) 57 (1), 289– 300. Retrieved from http://www.jstor.org/stable/2346101 .

Boon, L.I., Geraedts, V.J., Hillebrand, A., Tannemaat, M.R., Contarino, M.F., Stam, C.J., Berendse, H.W., 2019. A systematic review of MEG-based studies in Parkinson's disease: the motor system and beyond. Hum. Brain Mapp. 40 (9), 2827– 2848 . https://doi.org/10.1002/hbm.24562 .

Boon, L.I., Hillebrand, A., Dubbelink, K.T.O., Stam, C.J., Berendse, H.W., 2017. Changes in resting-state directed connectivity in cortico-subcortical networks correlate with cognitive function in Parkinson's disease. Clin. Neurophysiol. 128 (7), 1319– 1326 .

Boring, M.J., Jessen, Z.F., Wozny, T.A., Ward, M.J., Whiteman, A.C., Richardson, R.M., Ghuman, A.S., 2019. Quantitatively validating the efficacy of artifact suppression techniques to study the cortical consequences of deep brain stimulation with magnetoencephalography. Neuroimage 199, 366– 374 . https://doi.org/10.1016/j.neuroimage.2019.05.080 .

Brookes, M.J., Woolrich, M., Luckhoo, H., Price, D., Hale, J.R., Stephenson, M.C., Morris, P.G., 2011. Investigating the electrophysiological basis of resting state networks using magnetoencephalography. Proc. Natl. Acad. Sci. USA 108 (40), 16783–16788 . https://doi.org/10.1073/pnas.1112685108 .

Brookes, M.J., Woolrich, M.W., Barnes, G.R., 2012. Measuring functional connectivity in MEG: a multivariate approach insensitive to linear source leakage. Neuroimage 63 (2), 910– 920 . https://doi.org/10.1016/j.neuroimage.2012.03.048 .

Brown, P., 2003. Oscillatory nature of human basal ganglia activity: relationship to the pathophysiology of Parkinson's disease. Movement Disord. 18 (4), 357– 363 .

Brown, P., Williams, D., 2005. Basal ganglia local field potential activity: character and functional significance in the human. Clin. Neurophysiol. 116 (11), 2510– 2519 . https://doi.org/10.1016/j.clinph.2005.05.009 .

Cao, C., Li, D., Jiang, T., Ince, N.F., Zhan, S., Zhang, J., Sun, B., 2015. Resting state cortical oscillations of patients with Parkinson disease and with and without subthalamic deep brain stimulation: a magnetoencephalography study. J. Clin. Neurophysiol. 32 (2), 109– 118. . https://doi.org/10.1097/WNP.0000000000000137 Retrieved from http://www.ncbi.nlm.nih.gov/pubmed/25233246 [doi] .

Cao, C., Li, D., Zeng, K., Zhan, S., Huang, P., Li, X., Sun, B., 2018. Levodopa reduces the phase lag index of Parkinson's disease patients: a magnetoencephalographic study. Clin. EEG Neurosci. , 1550059418781693 https://doi.org/10.1177/1550059418781693 .

Cao, C.Y., Zeng, K., Li, D.Y., Zhan, S.K., Li, X.L., Sun, B.M., 2017. Modulations on cortical oscillations by subthalamic deep brain stimulation in patients with Parkinson disease: a MEG study. Neurosci Lett 636, 95– 100. Retrieved from http://www.ncbi.nlm.nih.gov/pubmed/27818350 S0304-3940(16)30848-5 [pii];10.1016/j.neulet.2016.11.009 [doi] .

Carrette, E., De Tiege, X., Op De Beeck, M., De Herdt, V., Meurs, A., Legros, B., Vonck, K., 2011. Magnetoencephalography in epilepsy patients carrying a vagus nerve stimulator. Epilepsy Res 93 (1), 44– 52 . https://doi.org/10.1016/j.eplepsyres.2010.10.011 .

Colclough, G.L., Brookes, M.J., Smith, S.M., Woolrich, M.W., 2015. A symmetric multivariate leakage correction for MEG connectomes. Neuroimage 117, 439– 448 . https://doi.org/10.1016/j.neuroimage.2015.03.071 .

Contarino, M.F., Bour, L.J., Verhagen, R., Lourens, M.A., de Bie, R.M., van den Munckhof, P., Schuurman, P.R., 2014. Directional steering: a novel approach to deep brain stimulation. Neurology 83 (13), 1163– 1169 . https://doi.org/10.1212/wnl.0000000000000823 .

DeLong, M.R., Wichmann, T., 2007. Circuits and circuit disorders of the basal ganglia. Arch. Neurol. 64 (1), 20– 24 . https://doi.org/10.1001/archneur.64.1.20 .

Deuschl, G., Schade-Brittinger, C., Krack, P., Volkmann, J., Schafer, H., Botzel, K., Voges, J., 2006. A randomized trial of deep-brain stimulation for Parkinson's disease. N. Engl. J. Med. 355 (9), 896– 908 . https://doi.org/10.1056/NEJMoa060281 .

Fimm, B., Heber, I.A., Coenen, V.A., Fromm, C., Noth, J., Kronenbuerger, M., 2009. Deep brain stimulation of the subthalamic nucleus improves intrinsic alertness in Parkinson's disease. Mov Disord 24 (11), 1613– 1620 . https://doi.org/10.1002/mds.22580 .

Goldenholz, D.M., Ahlfors, S.P., Hamalainen, M.S., Sharon, D., Ishitobi, M., Vaina, L.M., Stufflebeam, S.M., 2009. Mapping the signal-to-noise-ratios of cortical sources in magnetoencephalography and electroencephalography. Hum. Brain. Mapp. 30 (4), 1077– 1086 . https://doi.org/10.1002/hbm.20571 .

Gong, G., He, Y., Concha, L., Lebel, C., Gross, D.W., Evans, A.C., Beaulieu, C., 2009. Mapping anatomical connectivity patterns of human cerebral cortex using in vivo diffusion tensor imaging tractography. Cereb. Cortex 19 (3), 524– 536 . https://doi.org/10.1093/cercor/bhn102 .

Haller, M., Donoghue, T., Peterson, E., Varma, P., Sebastian, P., Gao, R., Voytek, B. (2018). Parameterizing neural power spectra. *bioRxiv*, 299859. Retrieved from https://www.biorxiv.org/content/biorxiv/early/2018/04/11/299859.full.pdf. doi:10.1101/299859.

Hammond, C., Bergman, H., Brown, P., 2007. Pathological synchronization in Parkinson's disease: networks, models and treatments. Trends Neurosci. 30 (7), 357–364.

Harmsen, I.E., Rowland, N.C., Wennberg, R.A., Lozano, A.M., 2018. Characterizing the effects of deep brain stimulation with magnetoencephalography: a review. Brain Stimul. 11 (3), 481–491. https://doi.org/10.1016/j.brs.2017.12.016.

Heinrichs-Graham, E., Kurz, M.J., Becker, K.M., Santamaria, P.M., Gendelman, H.E., Wilson, T.W., 2014. Hypersynchrony despite pathologically reduced beta oscillations in patients with Parkinson's disease: a pharmaco-magnetoencephalography study. J. Neurophysiol. 112 (7), 1739–1747. Retrieved from. http://www.ncbi.nlm.nih.gov/pubmed/25008416 doi:jn.00383.2014 [pii];10.1152/jn.00383.2014 [doi].

Helmich, R.C., 2018. The cerebral basis of Parkinsonian tremor: a network perspective. Mov. Disord. 33 (2), 219–231. https://doi.org/10.1002/mds.27224.

Hill, K.K., Campbell, M.C., McNeely, M.E., Karimi, M., Ushe, M., Tabbal, S.D., Perlmutter, J.S., 2013. Cerebral blood flow responses to dorsal and ventral STN DBS correlate with gait and balance responses in Parkinson's disease. Exp. Neurol. 241, 105–112. https://doi.org/10.1016/j.expneurol.2012.12.003.

Hillebrand, A., Barnes, G.R., 2005. Beamformer analysis of MEG data. Int. Rev. Neurobiol. 68, 149–171. https://doi.org/10.1016/s0074-7742(05)68006-3.

Hillebrand, A., Barnes, G.R., Bosboom, J.L., Berendse, H.W., Stam, C.J., 2012. Frequency-dependent functional connectivity within resting-state networks: an atlas-based MEG beamformer solution. Neuroimage 59 (4), 3909–3921.

Hillebrand, A., Fazio, P., de Munck, J.C., van Dijk, B.W., 2013. Feasibility of clinical magnetoencephalography (MEG) functional mapping in the presence of dental artefacts. Clin. Neurophysiol. 124 (1), 107–113. https://doi.org/10.1016/j.clinph.2012.06.013.

Hillebrand, A., Nissen, I., Ris-Hilgersom, I., Sijsma, N., Ronner, H., van Dijk, B., Stam, C., 2016a. Detecting epileptiform activity from deeper brain regions in spatially filtered

MEG data. Clin. Neurophysiol. 127 (8), 2766–2769.
Hillebrand, A., Singh, K.D., Holliday, I.E., Furlong, P.L., Barnes, G.R., 2005. A new approach to neuroimaging with magnetoencephalography. Hum. Brain Mapp. 25 (2), 199–211.
Hillebrand, A., Tewarie, P., van Dellen, E., Yu, M., Carbo, E.W., Douw, L., Stam, C.J., 2016b. Direction of information flow in large-scale resting-state networks is frequency-dependent. Proc. Natl. Acad. Sci. USA 113 (14), 3867–3872. https://doi.org/10.1073/pnas.1515657113.
Hipp, J.F., Hawellek, D.J., Corbetta, M., Siegel, M., Engel, A.K., 2012. Large-scale cortical correlation structure of spontaneous oscillatory activity. Nat. Neurosci. 15 (6), 884–890. https://doi.org/10.1038/nn.3101.
Hirschmann, J., Ozkurt, T.E., Butz, M., Homburger, M., Elben, S., Hartmann, C.J., Schnitzler, A., 2011. Distinct oscillatory STN-cortical loops revealed by simultaneous MEG and local field potential recordings in patients with Parkinson's disease. Neuroimage 55 (3), 1159–1168. Retrieved from. http://www.ncbi.nlm.nih.gov/pubmed/21122819 S1053-8119(10)01541-7 [pii];10.1016/j.neuroimage.2010.11.063 [doi].
Hirschmann, J., Ozkurt, T.E., Butz, M., Homburger, M., Elben, S., Hartmann, C.J., Schnitzler, A., 2013b. Differential modulation of STN-cortical and cortico-muscular coherence by movement and levodopa in Parkinson's disease. Neuroimage 68, 203–213. Retrieved from. http://www.ncbi.nlm.nih.gov/pubmed/23247184 S1053-8119(12)01148-2 [pii];10.1016/j.neuroimage.2012.11.036 [doi].
Jech, R., Ruzicka, E., Urgosik, D., Serranova, T., Volfova, M., Novakova, O., Mecir, P., 2006. Deep brain stimulation of the subthalamic nucleus affects resting EEG and visual evoked potentials in Parkinson's disease. Clin. Neurophysiol. 117 (5), 1017–1028. https://doi.org/10.1016/j.clinph.2006.01.009.
Kahan, J., Urner, M., Moran, R., Flandin, G., Marreiros, A., Mancini, L., Foltynie, T., 2014. Resting state functional MRI in Parkinson's disease: the impact of deep brain stimulation on 'effective' connectivity. Brain 137 (Pt 4), 1130–1144. https://doi.org/10.1093/brain/awu027.
Klimesch, W., Schack, B., Sauseng, P., 2005. The functional significance of theta and upper alpha oscillations. Exp. Psychol. 52 (2), 99–108. https://doi.org/10.1027/1618-3169.52.2.99.
Kühn, A.A., Kupsch, A., Schneider, G.H., Brown, P., 2006. Reduction in subthalamic 8–35Hz oscillatory activity correlates with clinical improvement in Parkinson's disease. Eur. J. Neurosci. 23 (7), 1956–1960.
Levy, R., Ashby, P., Hutchison, W.D., Lang, A.E., Lozano, A.M., Dostrovsky, J.O., 2002. Dependence of subthalamic nucleus oscillations on movement and dopamine in Parkinson's disease. Brain 125 (6), 1196–1209.
Little, S., Pogosyan, A., Neal, S., Zavala, B., Zrinzo, L., Hariz, M., Brown, P., 2013. Adaptive deep brain stimulation in advanced Parkinson disease. Ann. Neurol. 74 (3), 449–457. https://doi.org/10.1002/ana.23951.
Litvak, V., Jha, A., Eusebio, A., Oostenveld, R., Foltynie, T., Limousin, P., Brown, P., 2011. Resting oscillatory cortico-subthalamic connectivity in patients with Parkinson's disease. Brain 134 (Pt 2), 359–374. Retrieved from. http://www.ncbi.nlm.nih.gov/pubmed/21147836 awq332 [pii];10.1093/brain/awq332 [doi].
Louis, E.D., Tang, M.X., Cote, L., Alfaro, B., Mejia, H., Marder, K., 1999. Progression of parkinsonian signs in Parkinson disease. Arch. Neurol. 56 (3), 334–337.
Luoma, J., Pekkonen, E., Airaksinen, K., Helle, L., Nurminen, J., Taulu, S., Makela, J.P., 2018. Spontaneous sensorimotor cortical activity is suppressed by deep brain stimulation in patients with advanced Parkinson's disease. Neurosci. Lett. 683, 48–53. https://doi.org/10.1016/j.neulet.2018.06.041.
Maris, E., Oostenveld, R., 2007. Nonparametric statistical testing of EEG- and MEG-data. J. Neurosci. Methods 164 (1), 177–190. https://doi.org/10.1016/j.jneumeth.2007.03.024.
McGregor, M.M., Nelson, A.B., 2019. Circuit mechanisms of Parkinson's disease. Neuron 101 (6), 1042–1056. https://doi.org/10.1016/j.neuron.2019.03.004.
Medvedovsky, M., Taulu, S., Bikmullina, R., Ahonen, A., Paetau, R., 2009. Fine tuning the correlation limit of spatio-temporal signal space separation for magnetoencephalography. J. Neurosci. Methods 177 (1), 203–211. https://doi.org/10.1016/j.jneumeth.2008.09.035.
Mueller, K., Jech, R., Ruzicka, F., Holiga, S., Ballarini, T., Bezdicek, O., Urgosik, D., 2018. Brain connectivity changes when comparing effects of subthalamic deep brain stimulation with levodopa treatment in Parkinson's disease. Neuroimage Clin. 19, 1025–1035. https://doi.org/10.1016/j.nicl.2018.05.006.
Muthuraman, M., Hellriegel, H., Hoogenboom, N., Anwar, A.R., Mideksa, K.G., Krause, H., Raethjen, J., 2014. Beamformer source analysis and connectivity on concurrent EEG and MEG data during voluntary movements. PLoS One 9 (3), e91441. https://doi.org/10.1371/journal.pone.0091441.
Nambu, A., Tokuno, H., Takada, M., 2002. Functional significance of the cortico-subthalamo-pallidal 'hyperdirect' pathway. Neurosci. Res. 43 (2), 111–117. https://doi.org/10.1016/s0168-0102(02)00027-5.
Nichols, T.E., Holmes, A.P., 2002. Nonparametric permutation tests for functional neuroimaging: a primer with examples. Hum. Brain Mapp. 15 (1), 1–25.
Dubbelink, Olde, T., K., Stoffers, D., Deijen, J.B., Twisk, J.W., Stam, C.J., Berendse, H.W., 2013. Cognitive decline in Parkinson's disease is associated with slowing of resting-state brain activity: a longitudinal study. Neurobiol. Aging 34 (2), 408–418. Retrieved from. http://www.ncbi.nlm.nih.gov/pubmed/22495052 S0197-4580(12)00178-9 [pii];10.1016/j.neurobiolaging.2012.02.029 [doi].
Oswal, A., Beudel, M., Zrinzo, L., Limousin, P., Hariz, M., Foltynie, T., Brown, ..., 2016a. Deep brain stimulation modulates synchrony within spatially and spectrally distinct resting state networks in Parkinson's disease. Brain 139 (Pt 5), 1482–1496. Retrieved from. http://www.ncbi.nlm.nih.gov/pubmed/27017189 aww048 [pii];10.1093/brain/aww048 [doi].
Oswal, A., Jha, A., Neal, S., Reid, A., Bradbury, D., Aston, P., Litvak, V., 2016b. Analysis of simultaneous MEG and intracranial LFP recordings during deep brain stimulation: a protocol and experimental validation. J Neurosci Methods 261, 29–46. Retrieved from. http://www.ncbi.nlm.nih.gov/pubmed/26698227 S0165-0270(15)00432-X [pii];10.1016/j.jneumeth.2015.11.029 [doi].
Palva, S., Palva, J.M., 2012. Discovering oscillatory interaction networks with M/EEG: challenges and breakthroughs. Trends Cogn. Sci. 16 (4), 219–230. https://doi.org/10.1016/j.tics.2012.02.004.
Pellegrino, G., Maran, M., Turco, C., Weis, L., Di Pino, G., Piccione, F., Arcara, G., 2018. Bilateral transcranial direct current stimulation reshapes resting-state brain networks: a magnetoencephalography assessment. Neural Plast., 2782804. https://doi.org/10.1155/2018/2782804. *2018*.
Schoffelen, J.M., Gross, J., 2009. Source connectivity analysis with MEG and EEG. Hum. Brain Mapp. 30 (6), 1857–1865.
Silberstein, P., Pogosyan, A., Kühn, A.A., Hotton, G., Tisch, S., Kupsch, A., Brown, P., 2005. Cortico-cortical coupling in Parkinson's disease and its modulation by therapy. Brain 128 (6), 1277–1291.
Stoffers, D., Bosboom, J.L., Wolters, E.C., Stam, C.J., Berendse, H.W., 2008. Dopaminergic modulation of cortico-cortical functional connectivity in Parkinson's disease: an MEG study. Exp. Neurol. 213 (1), 191–195. Retrieved from. http://www.ncbi.nlm.nih.gov/pubmed/18590728 S0014-4886(08)00245-8 [pii];10.1016/j.expneurol.2008.05.021 [doi].
Taulu, S., Hari, R., 2009. Removal of magnetoencephalographic artifacts with temporal signal-space separation: demonstration with single-trial auditory-evoked responses. Hum. Brain Mapp. 30 (5), 1524–1534. https://doi.org/10.1002/hbm.20627.
Taulu, S., Simola, J., 2006. Spatiotemporal signal space separation method for rejecting nearby interference in MEG measurements. Phys Med Biol 51 (7), 1759–1768. https://doi.org/10.1088/0031-9155/51/7/008.
Tzourio-Mazoyer, N., Landeau, B., Papathanassiou, D., Crivello, F., Etard, O., Delcroix, N., Joliot, M., 2002. Automated anatomical labeling of activations in SPM using a macroscopic anatomical parcellation of the MNI MRI single-subject brain. Neuroimage 15 (1), 273–289. https://doi.org/10.1006/nimg.2001.0978.
Whalen, C., Maclin, E.L., Fabiani, M., Gratton, G., 2008. Validation of a method for coregistering scalp recording locations with 3D structural MR images. Hum Brain Mapp 29 (11), 1288–1301. https://doi.org/10.1002/hbm.20465.
Whitmer, D., de Solages, C., Hill, B., Yu, H., Henderson, J.M., Bronte-Stewart, H., 2012. High frequency deep brain stimulation attenuates subthalamic and cortical rhythms in Parkinson's disease. Front. Hum. Neurosci. 6, 155. https://doi.org/10.3389/fnhum.2012.00155.